Published in final edited form as:

Langmuir. 2019 June 11; 35(23): 7354–7363. doi:10.1021/acs.langmuir.8b02831.

Bulk droplet vitrification: an approach to improve large-scale hepatocyte cryopreservation outcome

Reinier J. de Vries[1,2,3], **Peony D. Banik**[1,2], **Sonal Nagpal**[1,2], **Lindong Weng**[1,2], **Sinan Ozer**[1,2], **Thomas M. van Gulik**[3], **Mehmet Toner**[1,2], **Shannon N. Tessier**[1,2,*], and **Korkut Uygun**[1,2,*]

[1]Department of Surgery, Massachusetts General Hospital, Boston, MA, USA. [2]Center for Engineering in Medicine, Harvard Medical School, Boston MA, USA. [3]Department of Surgery, University of Amsterdam, Amsterdam, the Netherlands.

Abstract

Loss of hepatocyte viability and metabolic function after cryopreservation is still a major issue. Although vitrification is a promising alternative, it has generally been proven to be unsuitable for vitrification of large cell volumes which is required for clinical applications. Here we propose a novel bulk droplet (3 to 5 mm diameter) vitrification method which allows high throughput volumes (4 ml/min), while using a low pre-incubated CPA concentration (15% v/v) to minimize toxicity and loss of cell viability and function. We used rapid (1.25 s) osmotic dehydration in order to concentrate a low pre-incubated intracellular CPA concentration ahead of vitrification, without the need of fully equilibrating toxic CPA concentrations. We compared direct post-preservation viability, long-term viability and metabolic function of bulk droplet vitrified, cryopreserved and fresh hepatocytes. Simulations and cooling rate measurements confirmed an adequate concentration of the intracellular CPA concentration (up to 8.53 M) after dehydration in combination with high cooling rates (960 to 1320°C/min) for successful vitrification. Compared to cryopreserved hepatocytes, bulk droplet vitrified hepatocytes had a significantly higher viability, directly after preservation and after one day in culture. Moreover, bulk droplet vitrified hepatocytes had evidently better morphology and showed significantly higher metabolic activity than cryopreserved hepatocytes in long term collagen sandwich cultures. In conclusion, we developed a novel bulk droplet vitrification method of which we validated the theoretical background and demonstrated the feasibility to use this method to vitrify large cell volumes. Moreover, we showed that this method results in improved hepatocyte viability and metabolic function as compared to cryopreservation.

Graphical Abstract

Corresponding authors: Drs. Shannon N. Tessier and Korkut Uygun, Communication should be addressed K.U., uygun.korkut@mgh.harvard.edu.

Author Contributions

The manuscript was written through contributions of all authors. All authors have given approval to the final version of the manuscript.

*co-corresponding author

Disclosures

The authors declare competing financial interests. Drs. Toner, de Vries and Tessier have provisional patent applications relevant to this study. Dr. Uygun has a financial interest in Organ Solutions, a company focused on developing organ preservation technology. Dr. Uygun's interests are managed by the MGH and Partners HealthCare in accordance with their conflict of interest policies.

Schematic representation of the bulk droplet vitrification method. Hepatocytes which are preincubated with a low CPA concentration (bright green) are rapidly mixed in a special mixing needle (blue/green serpentine lines) with a high CPA solution (bright blue). The mixing dehydrates the hepatocytes which concentrates the pre-incubated intracellular low CPA concentration. Hepatocyte droplets are generated by the mixing needle which are directly vitrified in liquid nitrogen before the high CPA concentration can diffuse over the cell membranes.

Keywords

Hepatocyte; Cryopreservation; Slow freezing; Droplet vitrification; Cryoprotectant agent

Introduction

End-stage liver disease claims over 30,000 lives in the US every year. Many patients become too ill to tolerate liver transplantation, and even if transplantation were a viable solution, there is a severe shortage of donor organs whereby only 28% of the wait-listed patients receive transplants[1]. As bioartificial liver assist devices (BAL) enter clinical trials[2–4], hepatocyte transplantation continues in clinical trials as an alternative treatment to liver failure[5], and whole-organ tissue engineering emerges as a vertical-advancement in the field[6–8], identifying suitable sources of hepatocytes is becoming an immediate issue[9]. For example, BAL devices require in the order of 10^{10} hepatocytes and up to 10^{9} hepatocytes are required per transplantation infusion, which must be highly viable to avoid potential harm to an already ill patient[4,10]. A major bottleneck in translating these ideally “off-the-shelf” cell-based treatment technologies to the clinic is the absence of a method to preserve them long enough for preparation and transportation to the patient site, without considerable loss of hepatocyte viability and function[11].

The classic method for cryopreservation is slow freezing after pre-incubation of one or more cryoprotectant agents (CPAs)[12,13]. When ice crystals form during the freezing process the CPA molecules are excluded from the growing ice lattice. The increasing CPA concentration of the extracellular liquid fraction causes an osmotic imbalance which dehydrates the cells during freezing of the sample. The resulting reduced intracellular aqueous volume leads to an increased intracellular concentration of the pre-incubated CPAs and both together reduce the chance of lethal intracellular ice formation. Nonetheless, CPA toxicity coupled with mechanical and osmotic stress of extracellular ice crystallization and recrystallization remain fundamental problems in cryopreservation. Despite many optimizations, after the first hepatocyte cryopreservation protocol was published in 1980[14], significant loss of viability and metabolic activity is still a major issue[4,10,15].

Vitrification poses the advantage by avoiding ice mediated injury altogether via a direct transition from the aqueous to the glass phase[12]. However, extremely fast cooling rates are required to reach the glass transition temperature while avoiding ice formation at higher subzero temperatures[16,17]. By addition of CPAs, the required critical cooling rate can be beneficially reduced, and the glass transition temperature increased[16]. Nonetheless, the required CPA concentrations are high, typically over 40% (v/v)[18]. To reach such high

concentrations, stepwise CPA introduction is used to reduce osmotic injury during CPA incubation[12]. Exposure of cells to permeable CPAs leads to fast (seconds) dehydration followed by slower (minutes) rehydration when CPAs, together with water, diffuse into the cells[19]. This effect is caused by the much faster diffusion rate of water over cell membranes as compared to CPAs. With each equilibration step taking several minutes, classical vitrification is a cumbersome and time-consuming technique which is practically constrained to simultaneous processing of few samples. Moreover, it considerably extends the exposure time of cells to high toxic CPA concentrations. Altogether, CPA toxicity is one of the key limitations of vitrification[20,21].

Although the critical cooling rate of aqueous solutions can be reduced by the addition of CPAs, extremely fast cooling rates of several hundred degrees per minute are nonetheless required for successful vitrification[17]. To obtain these high cooling rates, the samples must have small volumes (microliters) and large surface areas witnessed in the clinical usage of 0.5–2 mm diameter straws for vitrification of oocytes in liquid nitrogen. Although various alternative methods have been developed to increase the cooling rate and thus decrease the required CPA concentration[22–25], they rely on a small sample volume (i.e. the thermal mass) relative to the heat transfer area and are therefore intrinsically unsuitable for scale-up efforts to large volumes. A potential solution to this problem is droplet vitrification, whereby minuscule cell laden droplets are continuously dropped into liquid nitrogen. Previous research shows that the pre-incubated CPA concentration could be considerably reduced by using pico- to nanoliter sized droplets, resulting in high post vitrification cell viability[26–29]. Although arrays of droplet nozzles have been proposed, the extremely small droplet size and low throughput volumes still make this method unsuitable for scale up to bulk vitrification as is required for clinical application.

Here we present a novel bulk droplet vitrification technique, which allows vitrification of very large volumes of cells and droplets while allowing the use of low pre-incubated CPA concentrations. Using a brief osmotic dehydration seconds ahead of vitrification, we increased a low pre-incubated intracellular CPA concentration without the need of fully equilibrating high toxic CPAs concentrations. This was accomplished by loading low CPA pre-incubated hepatocytes into high CPA concentration droplets, instantaneously followed by exposure to liquid nitrogen. (Fig. 1) As such, we leveraged the rapid diffusion rate of water over cell membranes in comparison to CPAs. Moreover, the high extracellular CPA concentration allows the vitrification of magnitudes larger sized droplets (15–65μl) than other droplet vitrification approaches[26–29], enabling vitrification of bulk volumes. To our knowledge, this is the first introduction in literature of a high throughput (4ml/min), low toxicity method for vitrification which may result in a protocol viable for use in clinical hepatocyte therapy studies.

Methods

The aim of this study was to demonstrate the feasibility of our novel bulk droplet vitrification method and to use this new technique to improve primary hepatocyte preservation. To do this, we compared bulk droplet vitrification to the state-of-the-art cryopreservation protocol for hepatocyte cryopreservation. The cryopreservation protocols

which are most commonly used in literature involve controlled-rate slow freezing in modified University of Wisconsin (UW) solution. For the best results, UW is supplemented with either a mono or disaccharide (approx. 300 mM) and with DMSO (approx. 10% v/v) which is gradually added to avoid osmotic injury. All protocols include rapid thawing at 37°C followed by gradual dilution of DMSO at 4°C[30,31].

Experimental design

We compared bulk droplet vitrification of primary hepatocytes to the current best practice cryopreservation protocol and fresh controls. Primary rat hepatocytes from five different isolations (n=5 biological replicates) were divided across two experimental groups (bulk droplet vitrification and cryopreservation) and a fresh control group. Storage times varied from 2 to 8 days and were identical for the experimental groups within each biological replicate. Vitrification and cryopreservation were performed within 30 minutes of each other to ensure equal baseline viability between both groups. Direct post-preservation yield and viability were evaluated, and hepatocytes were cultured to assess plating efficiency and long-term viability and activity up to 7 days post-preservation.

Droplet size and temperature profile measurements

We experimentally confirmed droplet sizes and corresponding cooling rates. Droplets without hepatocytes were dropped in liquid nitrogen and collected as described below under ‘bulk droplet vitrification’. These vitrified droplets were divided on a circular black insulated plate with a diameter of 140mm (Fig 3a - **top**). A picture of the droplets was processed in ImageJ (National Institute of Health, Bethesda, Maryland) to measure the surface area relative to the known surface area of the plate (Fig 3a – **middle**).

To measure the droplet cooling rates, droplets were frozen at the tip of a thin (0.2 mm wire diameter) K-type thermocouple (Omega, Biel, Switzerland). Droplet size was controlled by incrementally freezing additional UW with CPAs on the existing droplet until the desired diameter was obtained. Next, the frozen droplets were rewarmed to 2°C-4°C and directly submerged in liquid nitrogen during which the temperature was logged at 100 ms intervals using a USB Thermocouple Data Acquisition Module (Omega, Biel, Switzerland) and Picolog 6 (Picotech, St. Neots, United Kingdom) software. The cooling temperature profiles of 3 mm and 5 mm droplets were measured three times per group. Additionally, we measured the cooling rate of the thermocouple without droplets to assess the thermocouple’s influence on the cooling rate of the droplets. Raw data was corrected for the offset of the thermocouple to the boiling point of liquid nitrogen.

Simulations

When exposed to a hypertonic solution of permeable CPAs, cells initially lose and then uptake water due to the change in osmotic gradient, accompanied by a constant influx of CPAs. Thus, cell morphology undergoes a shrink-and-swell behavior. The volumetric change as a function of time can be predicted by the K-K formalism[32].

$$dV/dt = -L_P ART\left[\left(m_s^e - m_s^i\right) + \sigma\left(m_c^e - m_c^i\right)\right] \quad (1)$$

$$dn_c/dt = (1-\sigma)(1/2)\left(m_c^e + m_c^i\right)dV/dt + P_s A\left(m_c^e - m_c^i\right) \quad (2)$$

In the above formalism, V is the cell volume, A the surface area and n_c the content of intracellular CPA. L_P is the hydraulic conductivity, P_S the membrane permeability to CPA and σ is the reflection coefficient. R is the gas constant and T the absolute temperature (277 K). m is the molality, with the superscripts denoting intracellular (i) and extracellular (e) and the subscripts denoting non-permeating salt (s) and permeating CPA (c), respectively. The used permeating CPAs during bulk droplet vitrification are DMSO and ethylene glycol (EG), as explained in detail under 'bulk droplet vitrification'. In our previous study, we have determined L_P (1.11 μm/atm/min), P_S (7.70 μm/min) and σ (0.581) for rat hepatocytes in exposure to DMSO at 4°C[19]. To simplify our calculation, we substituted DMSO for EG which will result in a small but acceptable deviance because the relative density difference is less than 1% and (DMSO 1.101 g/cm^3 vs EG 1.11 g/cm^3) and the size difference of the molecules is very small, assuming a hard sphere model (radius-DMSO 2.9 Angstrom vs radius-EG 2.18–2.44 Angstrom)[33,34]. We calculated $m_s^i = m_s^{i,0}\left(V_0 - V_b\right)/\left(V - V_b\right)$ and $m_c^i = n_c/\left(V - V_b\right)$ where V_0 is the isotonic cell volume, V_b the osmotically inactive volume (V_b/V_0=0.4061) and $m_s^{i,0}$ the isotonic salt concentration. The extracellular DMSO concentration in each CPA loading step is 1.175, 2.558 and 9.662 mol/kg, respectively, as approximately converted from the corresponding volume fraction (7.5%, 15% and 40% respectively). Equations (1) and (2) were solved in Matlab (The MathWorks, Inc., Natick, MA). This simulation was validated in our previous study using real time imaging of rat hepatocytes in a single cell entrapment microfluidic device during exposure to DMSO[19].

Animal care and hepatocyte isolation.

All animal protocols were approved by the Institutional Animal Care and Use Committee (IACUC) of Massachusetts General Hospital, Boston, Massachusetts, USA. Primary rat hepatocytes were isolated from female Lewis rat livers using the two-step collagenase perfusion technique[35].

Cryopreservation

We used the most widely accepted protocol for cryopreservation in literature. Fresh hepatocytes were spun down at 25 g for 5 minutes and resuspended in UW (Bridge to Life, Columbia, South-Carolina) supplemented with 2.2 mg/ml bovine serum albumin (Sigma-Aldrich, Boston, Massachusetts) and 333 mM glucose (Sigma-Aldrich). DMSO (Sigma-Aldrich) (5% v/v) was added in two steps with 3 minutes equilibration in between, resulting in a final cell density of 5×10^6/ml and a total pre-incubated CPA concentration of 10% v/v DMSO and 300 mM glucose. The hepatocyte suspension was transferred into four 1.5ml

cryovials (ColeParmer, Vernon Hills, Illinois) each containing 7.5×10^6 hepatocytes. Exactly 3 minutes after the last DMSO addition the vials were placed in a Cryomed™ controlled rate freezer (Thermo Fischer Scientific, Waltham, Massachusetts) and frozen to −140°C using the controlled rate freezing protocol as described elsewhere[31]. Upon completion, the cryovials were stored at −196°C until thawing.

After storage at −196°C for 2 to 8 days, the four cryovials were rapidly thawed in an agitated 37°C water bath. As soon as all ice was melted the content of the cryovials was added to 25 ml ice cold Dulbecco's Modified Eagle Medium (DMEM) (Sigma-Aldrich) supplemented with 300 mM glucose. After 3 minutes equilibration, the glucose concentration was diluted to 150 mM by addition of 25 ml ice cold DMEM. Subsequently, the cells were spun down for 5 minutes at 25 g and resuspended in 4 ml C+H culture medium (Cell Resource Core, Massachusetts General Hospital, Boston Massachusetts).

Bulk droplet vitrification

Fresh hepatocytes were spun down for 5 minutes at 25 g and resuspended in UW supplemented with 2.4 mg/ml BSA at 4°C. DMSO (3.75% v/v) and Ethylene Glycol (EG) (Sigma-Aldrich) (3.75% v/v) were added in two steps with an equilibration of 3 minutes between each step, resulting in a final cell density of $1e^7$/ml and a combined pre-incubated CPA concentration of 15%. During the last incubation period, the cells were laden in a 3 ml syringe and a second 3 ml syringe was laden with UW supplemented with 2 mg/ml BSA, 32.5% v/v DMSO, 32.5% v/v EG and 800 mM sucrose. The syringes were mounted into a custom 3D-printed syringe pump adapter that ensures even flowrates from both syringes. Next, a modified mixing needle (Grainger, Lake Forest, Illinois) (Fig. 2 **insert a**) was attached and the complete assembly was placed in the syringe pump (Pumpsystems Inc., Kernersville, North-Carolina). The syringe pump was mounted in vertical position to the wall of a tissue culture hood with the needle facing down toward the liquid nitrogen dewar (Thermo Fisher Scientific), as shown in Figure 2. A droplet collection assembly consisting of a funnel (Cole-Parmer) and 50 ml conical tube was placed in the liquid nitrogen dewar as shown in Figure 2, **insert b**. At the end of an incubation period of 3 minutes, the syringe pump was started at 2 ml/min, resulting in a high CPA exposure time of 1.25 seconds and a total droplet CPA concentration of 20% v/v DMSO, 20% v/v EG and 400mM sucrose. The mixing time is dependent on the total flow rate and volume of the mixing needle. Exactly 5 ml, i.e. 2.5×10^7 hepatocytes, was dropped in the liquid nitrogen and collected in the conical tube which was stored at −196°C until devitrification. For devitrification, the cell laden glass droplets were added to 100 ml warm (37°C) DMEM supplemented with 500 mM sucrose (Sigma-Aldrich) which was agitated for several seconds until the droplets were devitrified. The resulting cell suspension solution was divided into two 50 ml conical tubes which were spun down at 50 g for 2min. 37.5 ml was aspirated from both conical tubes and the sucrose concentration was gradually diluted to 125 mM by addition of 12.5 ml and 25.0 ml ice cold DMEM every 3 minutes, respectively. Next, the cells were spun down for 5 minutes at 25 g and resuspended and combined in 4 ml C+H culture medium.

Cell culture

Hepatocytes were cultured using a collagen sandwich culture model up to 7 days as described in detail elsewhere[36,37]. In short, the hepatocytes were seeded on 12 well precoated collagen plates (Thermo Fischer Scientific) with a seeding density of 1×10^6 and 9×10^5 hepatocytes per well for the experimental and fresh control groups respectively, to account for cell death after preservation. Nonattached hepatocytes were washed off one hour after seeding. Collagen top gel was added 24 hours after seeding. Media was changed in 24-hour intervals with a media volume of 0.5 ml per well. Aspirated media was stored at −80°C for post hoc analysis of urea production and albumin synthesis. Hepatocytes from experimental groups were cultured on the same plates to ensure equal culture conditions.

Evaluation of cell viability and activity

Assessment of post-preservation hepatocyte membrane integrity and yield— Membrane integrity of hepatocytes in suspension was measured using the standard trypan blue exclusion assay (Thermo Fisher Scientific), according to the manufacturer's instructions. Hepatocyte membrane integrity in suspension was measured during hepatocyte isolation, directly prior to and post cryopreservation and vitrification. The yield was calculated by dividing the total amount of live hepatocytes in suspension after preservation by 3.0×10^7 or 2.5×10^7, corresponding to the amount of liver cells that were cryopreserved and vitrified respectively. Fluorescent Hoechst/Propidium Iodide (PI) staining (Thermo Fisher Scientific) was used to measure the membrane integrity of hepatocytes one day after seeding to evaluate plating efficiency. Designated wells were incubated for 5 minutes with 3 μl/ml Hoechst and 10 μl/ml PI. Images were taken using an EVOS microscope (Thermo Fisher Scientific) with exposure times of 30 ms and 750 ms respectively. Images were quantified using ImageJ.

Assessment of metabolic hepatocyte activity—Reductive activity of hepatocytes in collagen sandwich cultures was measured using the Presto Blue essay (Thermo Fisher Scientific). On day 3, 5 and 7, 50 μl Presto blue was added to the media of designated wells. After a 30 minutes incubation, the fluorescence of 110 μL samples was measured on a Synergy-2™ micro plate reader (BioTek, Winooski, Vermont) according to the manufacturer's instructions.

Urea production—To measure the urea concentration in the culture media, a colorimetric BUN assay was performed with the use of the Stanbio™ BUN Diagnostic Set (Stanbio Laboratories, Cardiff, Wales) with the protocol provided by the manufacturer. Briefly, the urea assay reagent was prepared by mixing one part of the color reagent with two parts of the acid reagent. Standards were prepared and 10 μL of the standards or media samples were plated on a 96 well flat bottom plate, after which 150 μL of the urea reagent mixture was added. After an incubation at 60˚C for 90 minutes, the plate was allowed to cool down (5–10 min) and the absorbance was measured at 520 nm using a Benchmark Plus™ microplate spectrophotometer (Bio-Rad, Hercules, California)

Albumin synthesis—We measured rat serum albumin in the culture media using an enzyme-linked immunosorbent assay (ELISA) developed in-house. Briefly, high-binding 96

well ELISA plates were coated with rat albumin in PBS and incubated overnight at 4˚C. These plates were then washed four times with a 0.5% PBS-Tween solution. 50 μL of standards or media was added to the wells. After diluting 1:10,000 in PBS, peroxidase-conjugated albumin antibody was added to each well and incubated overnight at 4˚C/for 2 hours at 37˚C. Post incubation, the plates were washed again with 0.5% PBS-Tween. After preparation of o-Phenylenediamine dihydrochloride (400 mg/mL) and 4 uM hydrogen peroxide, 50 μL of the solution was added to each well and incubated for 5 minutes. The reaction was stopped with the addition of 50μL of 8 N sulfuric acid and the absorbance was measured at 490 nm to 650 nm on a Benchmark Plus™ microplate spectrophotometer.

Statistical analysis

Data were tested for normality using visual inspection and the Shapiro-Wilk normality test. Viability data of hepatocytes in suspension before and after preservation were compared using a paired one-way ANOVA with the Tukey correction for multiple testing. The Wilcoxon matched-pairs signed rank test was used to compare the preservation yields and although this data was not normally distributed, we used the F-test to compare the variance in yield. Culture data of fresh cells was corrected to a seeding density of 1 million cells per well to match the experimental groups. The paired Student's t-test was used to compare cell number and viability of monolayer cultured hepatocytes. Time-course data of the Presto Blue, urea and albumin assays were analyzed with paired repeated measures two-way ANOVAs with the Tukey correction for multiple testing. P-values <0.05 were considered statistically significant. All analyses were performed in Prism 7.03 (GraphPad Software Inc., La Jolla, California).

Results

Droplet size distribution and cooling rate

As shown in Figure 3a, the mean droplet diameter was 3.0 ± 1.0 mm (mean ± SD). The inverse Leidenfrost effect caused droplets to briefly levitate on the liquid nitrogen surface before submersion. We observed occasional merging of droplets during this phenomenon, resulting in a maximal observed droplet size of 4.4 mm. We measured the cooling rate of 3 mm and 5mm droplets to determine the mean and minimum cooling rate of the droplets (Fig 3b). Linear regression gave an average cooling rate of 1320 and 960°C/min respectively.

Simulations

We simulated the relative volume change of hepatocytes and the intracellular CPA concentration during CPA pre-incubation and subsequent short exposure to high CPA concentration in the mixing needle, as shown in Figure 3c and 3d. During the mixing time of 1.25 seconds, the dehydration reduces the intracellular volume to 59%. This results in an increase of the intracellular CPA concentration from 2.53 to 8.53 Mol/kg^{H2O}. Additionally, our simulations of cell volume during CPA pre-incubation show that a CPA equilibration period of 3 minutes is enough for hepatocytes to rehydrate to 95% of their initial size.

Post-preservation membrane integrity and yield

Cell membrane integrity is the most widely used metric to assess the quality of preserved cell suspensions. However, the percentage of cells with intact membranes can be paradoxically high if dying cells not only lose their membrane integrity but also disintegrate during preservation. Since this would result in a lower yield, it is important to also consider the preservation yield as an additional preservation parameter. Droplet vitrification resulted in significantly higher membrane integrity of hepatocytes in suspension than cryopreservation (79.0% ± 2.7% vs 67.4% ± 5.6%, p=0.044), as shown in Figure 4a. Moreover, the loss of membrane integrity compared to fresh controls was over two times larger during cryopreservation than during vitrification (mean differences with fresh controls of 22.0%, p=0.002 and 10.4%, p=0.0450 respectively). We did not observe a significant difference in preservation yield between cryopreservation and vitrification (47.6% ± 11.0% vs 57.64% ± 2.3%), as shown in Figure 4b. However, the yield of droplet vitrification was markedly more consistent as compared to cryopreservation, demonstrated by a significantly lower standard deviation (2.3% vs 11.0%, p=0.0108).

Hepatocyte plating efficiency (monolayer culture)

Although direct post-preservation cell membrane integrity is the most widely used metric for cell quality, it results in a potential overestimation of viability because some cells may experience delayed onset cell death. These cells have often lost functional properties such as attachment ability and commonly die within several hours after preservation. We addressed this potential problem by assessing the plating efficiency of cryopreserved and droplet vitrified hepatocytes. We evaluated plating efficiency by dead/live staining of hepatocytes in monoculture one day after preservation. (Fig. 5a) Although the difference between the total number of attached cryopreserved and droplet vitrified hepatocytes did not reach statistical significance (930 ± 263 vs 630 ± 327) (Fig. 5b), the mean number of attached hepatocytes was 48% higher after droplet vitrification (Fig 5c). More importantly, the membrane integrity of the attached hepatocytes after vitrification was significantly higher than after cryopreservation (92.3% ± 4.5% vs 81.92% ± 4.4%; p=0.022).

Long term hepatocyte cultures (collagen sandwich culture)

For most applications, high long-term viability and metabolic activity are of utmost importance. To study the long-term effects of preservation on hepatocyte viability and metabolic activity we cultured fresh, cryopreserved and droplet vitrified hepatocytes. The gold standard for primary hepatocyte culture is the collagen sandwich culture whereby the hepatocytes are seeded on collagen coated plates and covered by a collagen top gel 24 hours after seeding[38]. We cultured cells using the collagen sandwich model for a week and performed assays from day 2 onwards to allow the hepatocytes to adjust to the collagen top layer. Of note, we did not encounter any contamination issues after direct exposure of hepatocyte droplets to liquid nitrogen, which would have been revealed during a long-term culture.

Hepatocyte morphology—Fresh, cryopreserved and droplet vitrified hepatocytes developed a characteristic polygonal shaped monolayer with the presence of typical

binuclear cells on day 1 after plating, as shown in Figure 6a. The confluency of the cryopreserved hepatocytes was markedly lower compared to the fresh and vitrified hepatocytes which had similar confluency. On day 3, the hepatocytes of all groups had formed bile cuniculi, which is an important characteristic in collagen sandwich cultures. However, bile cuniculi in the cryopreserved group were less noticeable, as compared to fresh and droplet vitrified cultures, also when lower confluency was considered. Over the course of days, the visible number of dead cells increased in all groups, resulting in a slight reduction in confluency of the fresh and droplet vitrified hepatocytes and an evidently more reduced confluency of the cryopreserved hepatocytes.

Presto blue—We used the Presto Blue assay to evaluate the general cellular metabolic activity of hepatocytes in collagen sandwich cultures on day 3, 5 and 7 (Fig. 6b and Table 1). Reductive metabolic activity, measured in relative fluorescent units (RFU) of metabolized presto blue per 1×10^6 hepatocytes, of fresh hepatocytes was significantly higher on all measured days compared to cryopreserved hepatocytes and only on day 3 and 7 compared to vitrified hepatocytes. We did not observe a statistically significant difference between the reductive metabolic activity of droplet vitrified and cryopreserved hepatocytes.

Urea production—Detoxification is a vital function of the liver. Ammonia is an extremely toxic base which is produced during the deamination of amino acids. Hepatocytes almost exclusively metabolize ammonia into much less toxic urea. As such, urea production is one of the most common markers of specific hepatic function. We measured urea production of fresh, cryopreserved and droplet vitrified hepatocytes in collagen sandwich cultures by sampling the culture media over time for up to one week after preservation (Fig 7a and Table 1). From day 5 onwards, the urea production of vitrified hepatocytes was significantly higher than the urea production of cryopreserved hepatocytes. Fresh hepatocytes produced significantly more urea on every day compared to cryopreserved hepatocytes. However, in comparison to vitrified hepatocytes, the fresh hepatocytes only produces more urea on day 2, 3 and 7.

Albumin synthesis—Albumin is the most abundant blood protein which is almost exclusively produced by the liver. Therefore, it is considered the most important marker for synthetic metabolism of hepatocytes. We measured the albumin synthesis of fresh, cryopreserved and droplet vitrified hepatocytes in collagen sandwich cultures by sampling the culture media over time up to one week after preservation (Fig 7b and Table 1). On each day, the albumin synthesis of droplet vitrified hepatocytes was significantly higher than that of cryopreserved hepatocytes. On all days, fresh hepatocytes produced significantly more albumin than both cryopreserved and vitrified hepatocytes, except on day 5.

Discussion

Significant loss of hepatocyte viability and metabolic function after cryopreservation remains a major issue. This limitation severely throttles the use of hepatocytes in clinical applications such as BAL devices and hepatocyte transplantation, as well as their use in emerging tissue engineering approaches[4,39,40]. Although vitrification is a promising alternative to cryopreservation, the required rapid cooling rates in the traditional protocols

make it problematic to vitrify large cell volumes in the order of 10^{10} hepatocytes, as is required for clinical and tissue engineering applications[4,10]. To address this limitation, we proposed a novel bulk droplet vitrification method which allows true high throughput processing while using a low pre-incubated CPA concentration, with the overall goal to improve primary hepatocyte preservation.

Instrumental to our approach is the osmotic dehydration of hepatocytes which are pre-incubated with a low CPA concentration. This dehydration concentrated the intracellular CPAs just ahead of vitrification. Thereby, a sufficient intracellular CPA concentration was obtained without the need to fully equilibrate the toxic CPAs at high concentrations. We confirmed that a dehydration for 1.25 seconds sufficiently increases the pre-incubated intracellular CPA concentration, which in conjunction with the measured cooling rates of our large size droplets enables vitrification[17]. Compared to ultra-rapid cooling vitrification techniques we used similar pre-incubated low CPA concentrations (15% v/v) while achieving a much higher processing volume rates[22–25]. For example, compared to micro-droplet vitrification, we were able to use over ten thousand times larger droplets resulting in much higher volume processing rates[26–29].

Contamination is a potential issue when using an open method such as droplet vitrification. To prevent contamination, we used our system in a sterile laminar flow cell culture hood. Although the liquid nitrogen used was not sterile, we did not encounter any contamination issues which would been revealed during long term cultures. If required, liquid nitrogen can be sterilized by radiation or filtering[41].

Although high cooling rates are required for vitrification, it is well known that it is especially difficult to obtain high enough rewarming rates for successful devitrification[13,20]. Convective rewarming is traditionally used for devitrification. However, this outside in rewarming makes it difficult to reach sufficient rewarming rates in the sample cores. Although new inside out rewarming technologies such as electromagnetic warming of nanoparticles have recently been developed[42], they are technically complex and expensive solutions. In this regard, the devitrification of vitrified droplets in warm media has the additional advantage in which the outer already devitrified layer is replaced by warm media. This reduces the thermal resistance to the core and the thermal mass of the droplet, significantly increasing the rewarming rate.

To study the effects of bulk droplet vitrification on primary hepatocyte viability and the potential improvement over cryopreservation, we compared direct post-preservation parameters after bulk droplet vitrification with the most commonly used cryopreservation protocol[30,31]. With this cryopreservation protocol, reductions in absolute viability between 15 to 25% have been reported[43–45], which is comparable to our observed 22% loss of viability after cryopreservation in this study.

When comparing cryopreservation versus our new bulk droplet vitrification approach, loss of hepatocyte viability assessed by membrane integrity testing was about half after droplet vitrification as compared to cryopreservation (10% vs 22%). Yield, defined as the ratio between the total number of live cells after and before preservation, is another important

parameter of preservation efficiency which is often not reported in literature. We observed a 10% higher yield after droplet vitrification, although this did not reach statistical significance. However, it should be noted that there was a significantly more consistent yield after droplet vitrification, which may be important for clinical applications. Furthermore, it is well acknowledged that the attachment ability of hepatocytes is reduced after cryopreservation, resulting in lower plating efficiency[46]. Therefore, we compared the plating efficiency of hepatocytes in a monolayer 24 hours after seeding. Although not statistically significant, the attachment after droplet vitrification was nearly 50% higher than after cryopreservation. More importantly, the viability of the hepatocytes that did attach was 10% higher after vitrification. This difference is especially important when considering clinical applications; the lower delayed onset cell death after bulk droplet vitrification might result in a more effective therapy with BAL devices and hepatocyte transplantation, with fewer side effects due to remnants of dead hepatocytes.

Since long-term viability and metabolic activity is paramount for clinical and tissue engineering applications, we also assessed the effect of cryopreservation and droplet vitrification on hepatocyte viability and metabolic activity in collagen sandwich cultures up to one week after preservation. Based on phase-contrast images, the droplet vitrified hepatocytes had comparable morphology to fresh plated hepatocytes. It should be noted that the fresh hepatocytes were seeded at a lower density than both droplet vitrified and cryopreserved hepatocytes to correct for cell death after preservation. More importantly, the droplet vitrified hepatocytes clearly showed better morphology and confluency than cryopreserved hepatocytes.

Loss of metabolic activity after cryopreservation is an important problem after cryopreservation of hepatocytes[30], with negative consequences for clinical applications[4,40]. Like others, we observed lower metabolic activity after cryopreservation as compared to fresh cultured hepatocytes, demonstrated by both general and liver specific markers of metabolic activity. Bulk droplet vitrified hepatocytes had a significantly higher metabolic activity as compared to cryopreserved hepatocytes, based on a significantly higher urea production and albumin synthesis up to one week after preservation.

In conclusion, we have developed a novel bulk droplet vitrification method of which we validated the theoretical background and demonstrated the feasibility to use this method to vitrify large cell volumes. Moreover, we showed that this method results in improved hepatocyte viability and metabolic function as compared to cryopreservation. Future optimization of bulk droplet vitrification may improve the preservation yield and could potentially improve preservation of human primary hepatocytes. In particular, we expect that the pre-incubated CPA concentration could be reduced if the osmotic dehydration prior to vitrification is further optimized, whereby both permeable and non-permeable CPAs should be tested. Also, we propose scaling up to large (>1 liter) processing volumes with continuous fluidic low CPA pre-incubation. Since bulk droplet vitrification does not need specialized equipment such as a controlled rate freezer or microdroplet ejector nozzles, it is a simple and cost-effective preservation method which could potentially also be used for preservation of other cell types.

ACKNOWLEDGEMENTS

Funding from the US National Institutes of Health (R01DK096075, R01DK107875, and R01DK114506), the Department of Defense (DoD RTRP W81XWH-17-1-0680) and the Shriners Hospitals for Children is gratefully acknowledged.

Funding Sources

US National Institutes of Health (R01DK096075, R01DK107875, and R01DK114506)

US Department of Defense (DoD RTRP W81XWH-17-1-0680)

ABBREVIATIONS

BAL	Bioartificial Liver assist device
BSA	Bovine Serum Albumin
BUN	Blood Urea Nitrogen
CPA	Cryoprotectant agent
DMEM	Dulbecco's Modified Eagle Medium
DMSO	Dimethyl Sulfoxide
EG	Ethylene Glycol
ELISA	enzyme-linked immunosorbent assay
PBS	phosphate buffered saline
PI	propidium iodide
RFU	relative fluorescence units
SD	standard deviation

REFERENCES

(1). URL Optn.transplant.hrsa.gov (Accessed 20 November, 2012).

(2). Demetriou AA; Brown RS; Busuttil RW; Fair J; McGuire BM; Rosenthal P; Am Esch JS; Lerut J; Nyberg SL; Salizzoni M; et al. Prospective, Randomized, Multicenter, Controlled Trial of a Bioartificial Liver in Treating Acute Liver Failure. Ann. Surg 2004, 239 (5), 660–667; discussion 667–670. [PubMed: 15082970]

(3). Sorodoc L; Lionte C; Sorodoc V; Petris O; Jaba I Is MARS System Enough for A. Phalloides-Induced Liver Failure Treatment? Hum. Exp. Toxicol 2010, 29 (10), 823–832. [PubMed: 20179021]

(4). Carpentier B; Gautier A; Legallais C Artificial and Bioartificial Liver Devices: Present and Future. Gut 2009, 58 (12), 1690–1702. [PubMed: 19923348]

(5). Fitzpatrick E; Mitry RR; Dhawan A Human Hepatocyte Transplantation: State of the Art. J. Intern. Med 2009, 266 (4), 339–357. [PubMed: 19765179]

(6). Uygun BE; Soto-Gutierrez A; Yagi H; Izamis M-L; Guzzardi MA; Shulman C; Milwid J; Kobayashi N; Tilles A; Berthiaume F; et al. Organ Reengineering through Development of a Transplantable Recellularized Liver Graft Using Decellularized Liver Matrix. Nat. Med 2010, 16 (7), 814–820. [PubMed: 20543851]

(7). Petersen TH; Calle EA; Zhao L; Lee EJ; Gui L; Raredon MB; Gavrilov K; Yi T; Zhuang ZW; Breuer C; et al. Tissue-Engineered Lungs for in Vivo Implantation. Science 2010, 329 (5991), 538–541. [PubMed: 20576850]

(8). Ott HC; Matthiesen TS; Goh S-K; Black LD; Kren SM; Netoff TI; Taylor DA Perfusion-Decellularized Matrix: Using Nature's Platform to Engineer a Bioartificial Heart. Nat. Med 2008, 14 (2), 213–221. [PubMed: 18193059]

(9). Haridass D; Narain N; Ott M Hepatocyte Transplantation: Waiting for Stem Cells: Curr. Opin. Organ Transplant 2008, 13 (6), 627–632. [PubMed: 19060554]

(10). Hughes RD; Mitry RR; Dhawan A Current Status of Hepatocyte Transplantation: Transplantation 2012, 93 (4), 342–347. [PubMed: 22082820]

(11). Cell Injury: Mechanisms, Responses, and Repair; [Result of a Seminar Series Entitled Cell Injury: Responses and Repair Held between March 31st and Juni 2nd, 2004 at the University of Chicago, Chicago Illinois]; Lee RC, Seminar Series Entitled Cell Injury: Responses and Repair, Eds.; Annals of the New York Academy of Sciences; New York Academy of Sciences: New York, N.Y, 2005.

(12). Pegg DE Principles of Cryopreservation. Methods Mol. Biol. Clifton NJ 2007, 368, 39–57.

(13). Baust JG; Gao D; Baust JM Cryopreservation: An Emerging Paradigm Change. Organogenesis 2009, 5 (3), 90–96. [PubMed: 20046670]

(14). Fuller B; Morris G; Nutt L; Attenburrow V Functional Recovery of Isolated Rat Hepatocytes upon Thawing from −196 Degrees C. Cryo-Lett 1980, 1, 139–146.

(15). Fox IJ; Chowdhury JR Hepatocyte Transplantation: Hepatocyte Transplantation. Am. J. Transplant 2004, 4, 7–13.

(16). Fahy GM; MacFarlane DR; Angell CA; Meryman HT Vitrification as an Approach to Cryopreservation. Cryobiology 1984, 21 (4), 407–426. [PubMed: 6467964]

(17). Hopkins JB; Badeau R; Warkentin M; Thorne RE Effect of Common Cryoprotectants on Critical Warming Rates and Ice Formation in Aqueous Solutions. Cryobiology 2012, 65 (3), 169–178. [PubMed: 22728046]

(18). Fahy GM; Wowk B; Wu J; Phan J; Rasch C; Chang A; Zendejas E Cryopreservation of Organs by Vitrification: Perspectives and Recent Advances. Cryobiology 2004, 48 (2), 157–178. [PubMed: 15094092]

(19). Weng L; Ellett F; Edd J; Wong KHK; Uygun K; Irimia D; Stott SL; Toner M A Highly-Occupied, Single-Cell Trapping Microarray for Determination of Cell Membrane Permeability. Lab. Chip 2017, 17 (23), 4077–4088. [PubMed: 29068447]

(20). Pegg DE Principles of Cryopreservation. Methods Mol. Biol. Clifton NJ 2007, 368, 39–57.

(21). Best BP Cryoprotectant Toxicity: Facts, Issues, and Questions. Rejuvenation Res 2015, 18 (5), 422–436. [PubMed: 25826677]

(22). Shi M; Ling K; Yong KW; Li Y; Feng S; Zhang X; Pingguan-Murphy B; Lu TJ; Xu F High-Throughput Non-Contact Vitrification of Cell-Laden Droplets Based on Cell Printing. Sci. Rep 2016, 5 (1).

(23). He X; Park EYH; Fowler A; Yarmush ML; Toner M Vitrification by Ultra-Fast Cooling at a Low Concentration of Cryoprotectants in a Quartz Micro-Capillary: A Study Using Murine Embryonic Stem Cells. Cryobiology 2008, 56 (3), 223–232. [PubMed: 18462712]

(24). Kuwayama M Highly Efficient Vitrification for Cryopreservation of Human Oocytes and Embryos: The Cryotop Method. Theriogenology 2007, 67 (1), 73–80. [PubMed: 17055564]

(25). Heo YS; Nagrath S; Moore AL; Zeinali M; Irimia D; Stott SL; Toth TL; Toner M "Universal" vitrification of Cells by Ultra-Fast Cooling. TECHNOLOGY 2015, 03 (01), 64–71.

(26). Demirci U; Montesano G Cell Encapsulating Droplet Vitrification. Lab. Chip 2007, 7 (11), 1428. [PubMed: 17960267]

(27). El Assal R; Guven S; Gurkan UA; Gozen I; Shafiee H; Dalbeyler S; Abdalla N; Thomas G; Fuld W; Illigens BMW; et al. Bio-Inspired Cryo-Ink Preserves Red Blood Cell Phenotype and Function During Nanoliter Vitrification. Adv. Mater 2014, 26 (33), 5815–5822. [PubMed: 25047246]

(28). Dou R; Saunders RE; Mohamet L; Ward CM; Derby B High Throughput Cryopreservation of Cells by Rapid Freezing of Sub-Ml Drops Using Inkjet Printing--Cryoprinting. Lab. Chip 2015, 15 (17), 3503–3513. [PubMed: 26190571]

(29). Samot J; Moon S; Shao L; Zhang X; Xu F; Song Y; Keles HO; Matloff L; Markel J; Demirci U Blood Banking in Living Droplets. PloS One 2011, 6 (3), e17530. [PubMed: 21412411]

(30). Stéphenne X; Najimi M; Sokal EM Hepatocyte Cryopreservation: Is It Time to Change the Strategy? World J. Gastroenterol 2010, 16 (1), 1–14. [PubMed: 20039443]

(31). Terry C; Dhawan A; Mitry RR; Lehec SC; Hughes RD Optimization of the Cryopreservation and Thawing Protocol for Human Hepatocytes for Use in Cell Transplantation. Liver Transpl 2010, 16 (2), 229–237. [PubMed: 20104500]

(32). Kedem O; Katchalsky A Thermodynamic Analysis of the Permeability of Biological Membranes to Non-Electrolytes. Biochim. Biophys. Acta 1958, 27 (2), 229–246. [PubMed: 13522722]

(33). Schrader AM; Donaldson SH; Song J; Cheng C-Y; Lee DW; Han S; Israelachvili JN Correlating Steric Hydration Forces with Water Dynamics through Surface Force and Diffusion NMR Measurements in a Lipid-DMSO-H2O System. Proc. Natl. Acad. Sci. U. S. A 2015, 112 (34), 10708–10713. [PubMed: 26261313]

(34). Tang KES; Bloomfield VA Excluded Volume in Solvation: Sensitivity of Scaled-Particle Theory to Solvent Size and Density. Biophys. J 2000, 79 (5), 2222–2234. [PubMed: 11053104]

(35). Seglen PO Preparation of Isolated Rat Liver Cells. Methods Cell Biol 1976, 13, 29–83. [PubMed: 177845]

(36). Dunn JC; Yarmush ML; Koebe HG; Tompkins RG Hepatocyte Function and Extracellular Matrix Geometry: Long-Term Culture in a Sandwich Configuration. FASEB J. Off. Publ. Fed. Am. Soc. Exp. Biol 1989, 3 (2), 174–177.

(37). Sosef MN; Baust JM; Sugimachi K; Fowler A; Tompkins RG; Toner M Cryopreservation of Isolated Primary Rat Hepatocytes: Enhanced Survival and Long-Term Hepatospecific Function. Ann. Surg 2005, 241 (1), 125–133. [PubMed: 15622000]

(38). Dunn JC; Tompkins RG; Yarmush ML Long-Term in Vitro Function of Adult Hepatocytes in a Collagen Sandwich Configuration. Biotechnol. Prog 1991, 7 (3), 237–245. [PubMed: 1367596]

(39). Sakiyama R; Blau BJ; Miki T Clinical Translation of Bioartificial Liver Support Systems with Human Pluripotent Stem Cell-Derived Hepatic Cells. World J. Gastroenterol 2017, 23 (11), 1974. [PubMed: 28373763]

(40). Pless G Artificial and Bioartificial Liver Support. Organogenesis 2007, 3 (1), 20–24. [PubMed: 19279696]

(41). Parmegiani L; Accorsi A; Cognigni GE; Bernardi S; Troilo E; Filicori M Sterilization of Liquid Nitrogen with Ultraviolet Irradiation for Safe Vitrification of Human Oocytes or Embryos. Fertil. Steril 2010, 94 (4), 1525–1528. [PubMed: 19591992]

(42). Manuchehrabadi N; Gao Z; Zhang J; Ring HL; Shao Q; Liu F; McDermott M; Fok A; Rabin Y; Brockbank KGM; et al. Improved Tissue Cryopreservation Using Inductive Heating of Magnetic Nanoparticles. Sci. Transl. Med 2017, 9 (379).

(43). Wang X; Magalhães R; Wu Y; Wen F; Gouk SS; Watson PF; Yu H; Kuleshova LL Development of a Modified Vitrification Strategy Suitable for Subsequent Scale-up for Hepatocyte Preservation. Cryobiology 2012, 65 (3), 289–300. [PubMed: 22940432]

(44). Jitraruch S; Dhawan A; Hughes RD; Filippi C; Lehec SC; Glover L; Mitry RR Cryopreservation of Hepatocyte Microbeads for Clinical Transplantation. Cell Transplant 2017, 26 (8), 1341–1354. [PubMed: 28901189]

(45). Arikura J; Kobayashi N; Okitsu T; Noguchi H; Totsugawa T; Watanabe T; Matsumura T; Maruyama M; Kosaka Y; Tanaka N; et al. UW Solution: A Promising Tool for Cryopreservation of Primarily Isolated Rat Hepatocytes. J. Hepatobiliary. Pancreat. Surg 2002, 9 (6), 742–749. [PubMed: 12658410]

(46). Guillouzo A; Rialland L; Fautrel A; Guyomard C Survival and Function of Isolated Hepatocytes after Cryopreservation. Chem. Biol. Interact 1999, 121 (1), 7–16. [PubMed: 10418967]

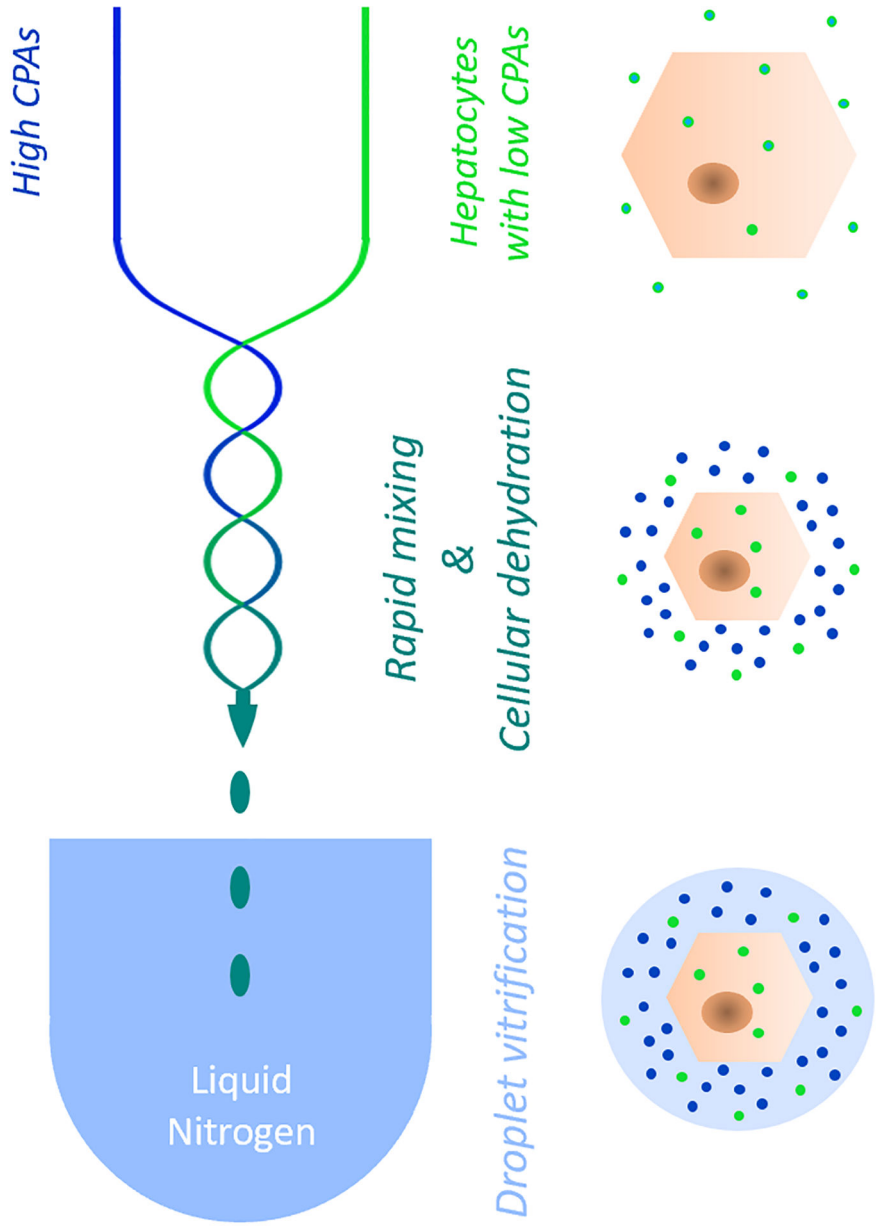

Figure 1.

Schematic representation of the bulk droplet vitrification method. Hepatocytes which are preincubated with a low CPA concentration (bright green) are rapidly mixed in a special mixing needle (blue/green serpentine lines) with a high CPA solution (bright blue). The mixing dehydrates the hepatocytes which concentrates the pre-incubated intracellular low CPA concentration. Hepatocyte droplets are generated by the mixing needle which are directly vitrified in liquid nitrogen before the high CPA concentration can diffuse over the cell membranes.

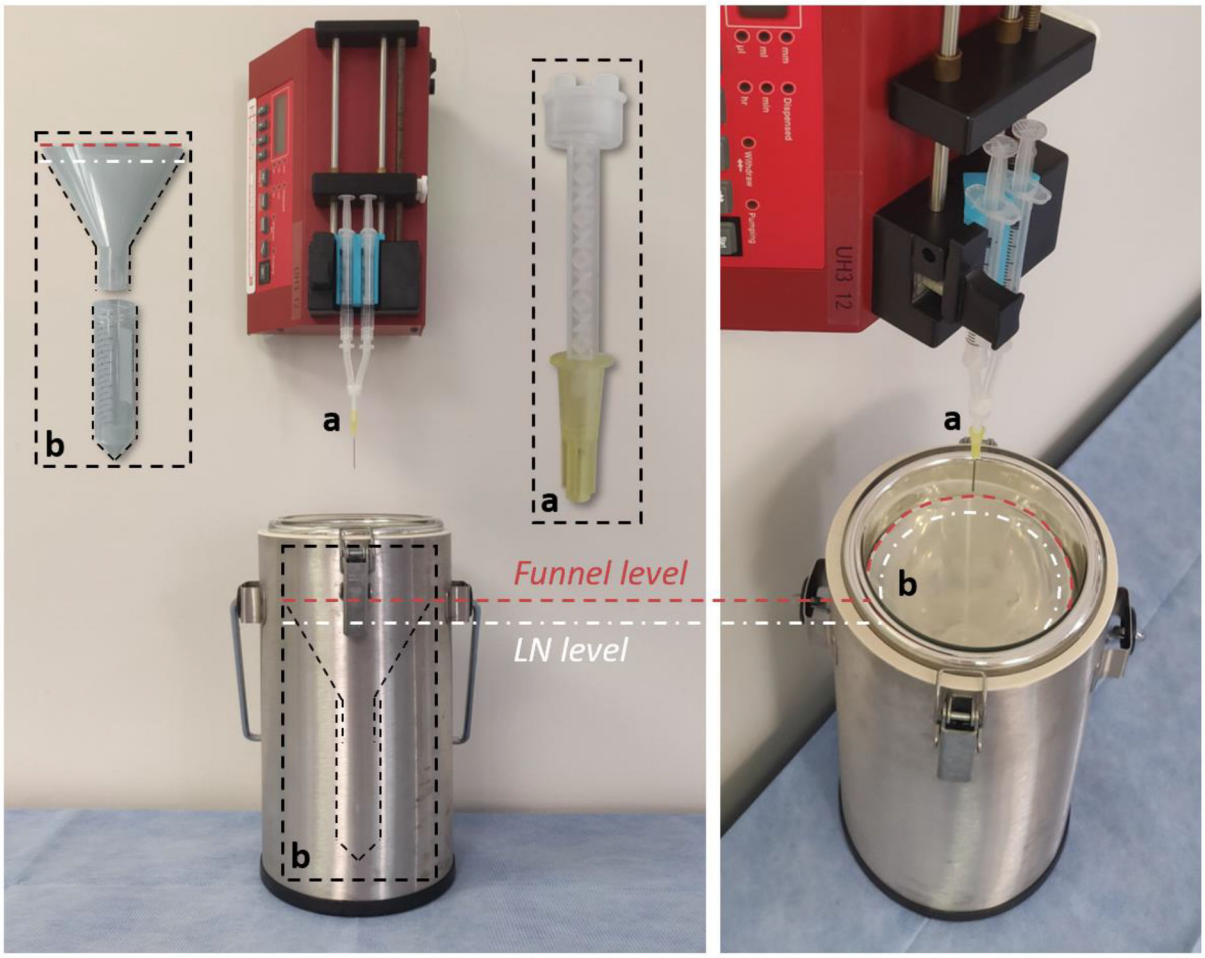

Figure 2.

Bulk droplet vitrification experimental setup. **Insert a**: detail of the mixing needle. **Insert b**: droplet collection device which is placed in the liquid nitrogen dewar.

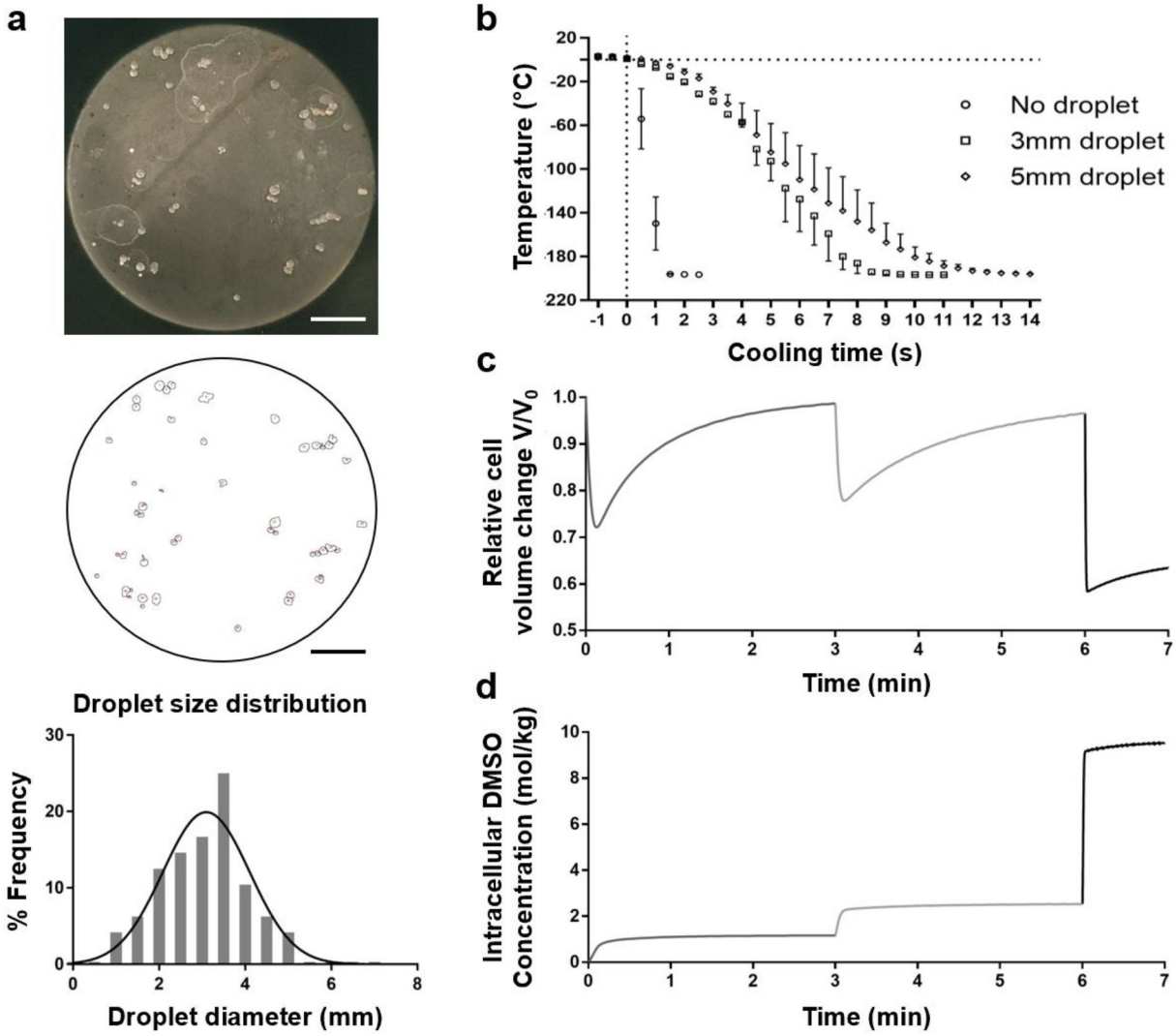

Figure 3.

Characterization of the bulk droplet vitrification method: droplet size, cooling rate, and cryoprotectant agent (CPA) loading. **a**. Droplet size measurements. Top: picture of vitrified droplets which do not contain hepatocytes. Middle: Image after particle analysis in ImageJ. The small circles correspond to the droplet circumferences. Below: Droplet size distribution **b**. Droplet temperature after exposure to liquid nitrogen at t=0 seconds. **c**. Relative volume change of hepatocytes during CPA incubation with exposure to 7.5% (v/v) dimethyl sulfoxide (DMSO) from 0–3 minutes, 15% (v/v) DMSO from 3–6 minutes and 40% (v/v) DMSO with 400mM sucrose from 6–7 minutes. **d**. Intracellular DMSO concentration during CPA incubation. Scale bars: 25 mm. Error bars: SD.

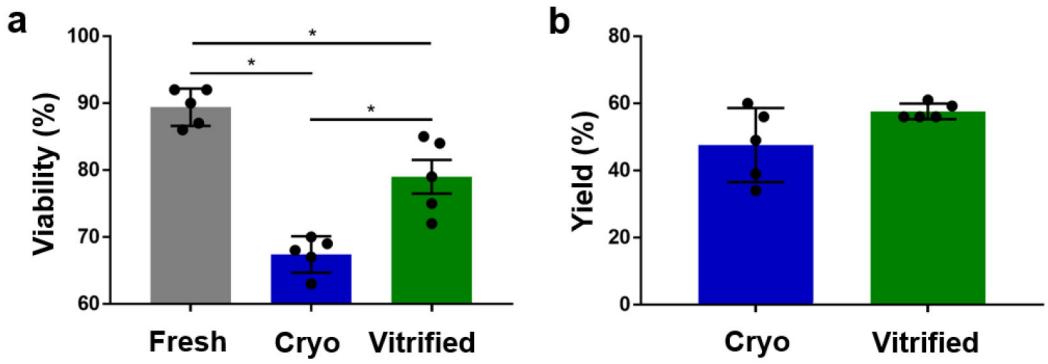

Figure 4.

Direct post-preservation viability and yield of cryopreserved (blue) and bulk droplet vitrified (green) hepatocytes in suspension. **a**. Viability. **b**. Yield. Stars: $p<0.05$ Error bars: SD.

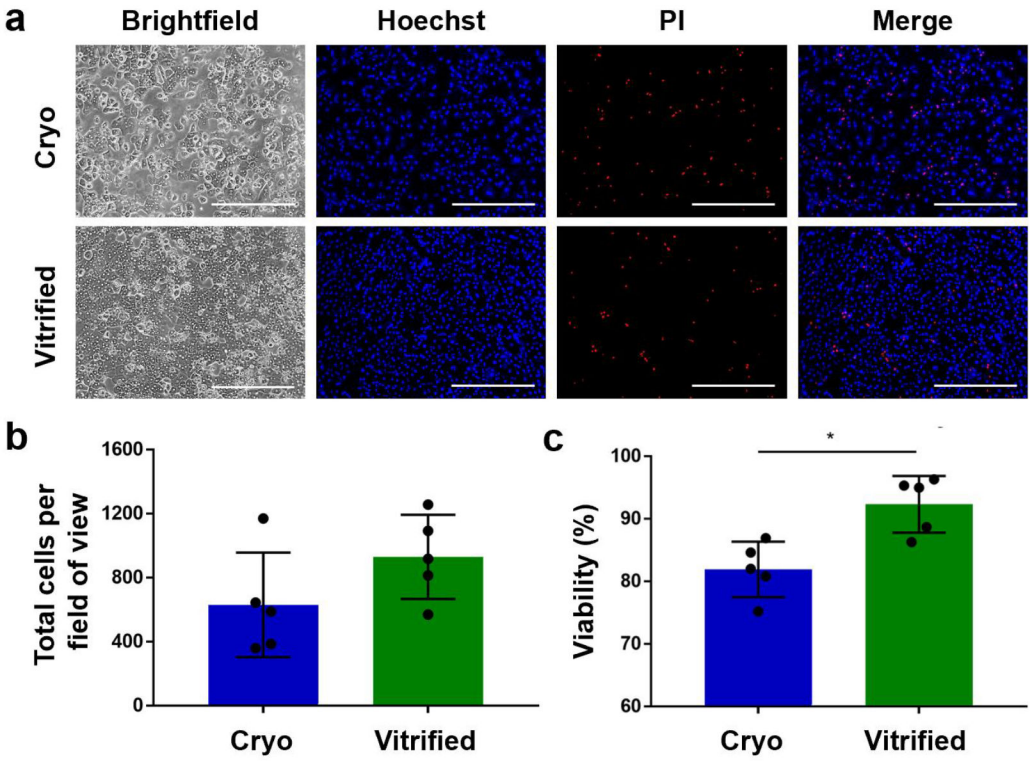

Figure 5.

Viability of cryopreserved (blue) and bulk droplet vitrified (green) hepatocytes after 24 hours monolayer culture. **a**. Representative images of Hoechst (all hepatocytes) / propidium iodide (PI) (dead hepatocytes) staining of the cultures. **b**. Total number of attached hepatocytes per field of view. **c**. Viability of attached hepatocytes. Scale bars: 400μm. Stars: $p<0.05$ Error bars: SD.

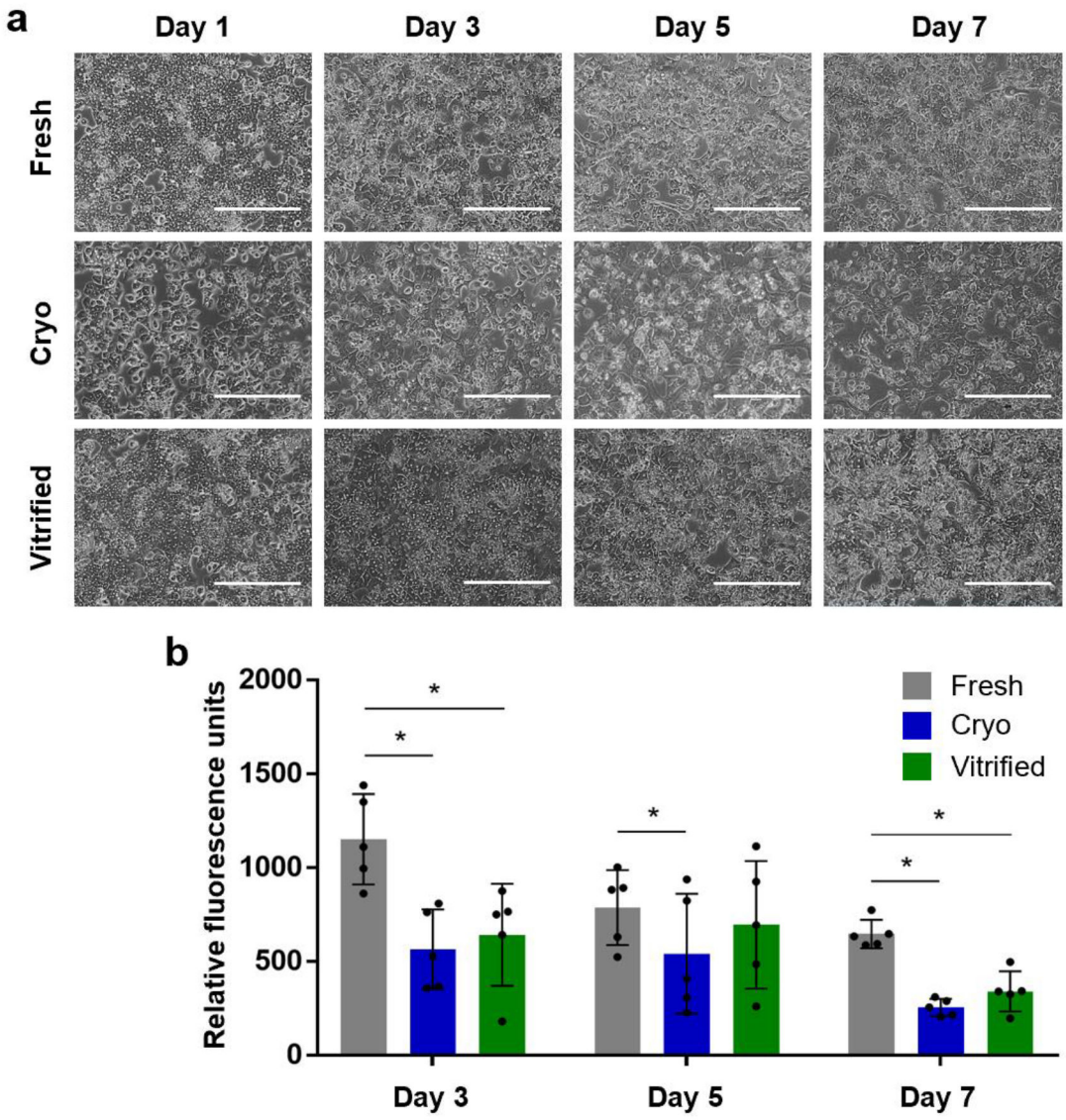

Figure 6.

Long-term collagen sandwich cultures of fresh (grey), cryopreserved (blue) and bulk droplet vitrified (green) hepatocytes. **a**. Representative microscopy images of fresh, cryopreserved and bulk droplet vitrified hepatocytes. **b**. Metabolic reduction activity of Presto Blue in collagen sandwich culture. Scale bars: 400μm. Stars: $p<0.05$ Error bars: SD.

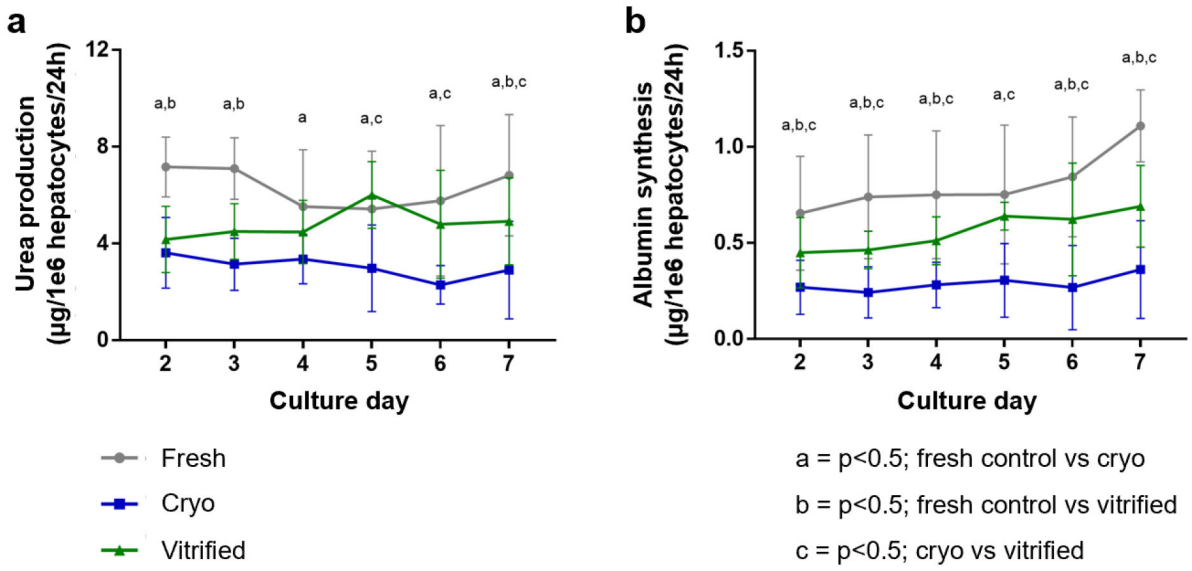

Figure 7.

Hepatic function during long-term collagen sandwich cultures of fresh (grey), cryopreserved (blue) and bulk droplet vitrified (green) hepatocytes. **a**. Urea production. **b**. Albumin synthesis. Letters: $p<0.05$; a: fresh vs cryopreserved; b: fresh vs bulk droplet vitrified; c: cryopreserved vs bulk droplet vitrified. Error bars: SD.

Table 1:

Metabolic activity of fresh, cryopreserved and bulk droplet vitrified hepatocytes in long-term collagen sandwich cultures.

		Fresh	Cryo	Vitrified	P values		
		Mean ± SD	***Mean ± SD***	***Mean ± SD***	***Fresh-Cryo***	***Fresh-Vitrified***	***Cryo-Vitrified***
Presto Blue	*Day 3*	1152 ± 241	565 ± 213	643 ± 271	<0.001	<0.001	0.660
	Day 5	787 ± 200	541 ± 319	696 ± 339	0.033	0.569	0.214
Units: RFU	*Day 7*	647 ± 76	255 ± 46	341 ± 107	0.001	0.008	0.606
Urea production	*Day 2*	7.2 ± 1.2	3.6 ± 1.5	4.2 ± 1.4	<0.001	<0.001	0.693
	Day 3	7.1 ± 1.3	3.1 ± 1.1	4.5 ± 1.1	<0.001	0.001	0.122
Units: μg/1e6 hepatocytes/24hr	*Day 4*	5.5 ± 2.6	3.6 ± 1.0	4.5 ± 1.3	0.007	0.271	0.232
	Day 5	5.4 ± 2.4	3.0 ± 1.8	6.0 ± 1.4	0.002	0.665	<0.001
	Day 6	5.8 ± 3.1	2.3 ± 0.8	4.8 ± 2.2	<0.001	0.326	0.002
	Day 7	6.8 ± 2.5	2.9 ± 2.0	4.9 ± 1.8	<0.001	0.019	0.013
Albumin synthesis	*Day 2*	0.65 ± 0.30	0.27 ± 0.14	0.45 ± 0.18	<0.001	0.019	0.045
	Day 3	0.74 ± 0.32	0.24 ± 0.13	0.46 ± 0.01	<0.001	0.001	0.011
Units: μg/1e6 hepatocytes/24hr	*Day 4*	0.75 ± 0.33	0.28 ± 0.12	0.51 ± 0.12	<0.001	0.006	0.008
	Day 5	0.75 ± 0.36	0.31 ± 0.19	0.64 ± 0.07	<0.001	0.284	<0.001
	Day 6	0.84 ± 0.31	0.27 ± 0.22	0.62 ± 0.29	<0.001	0.011	<0.001
	Day 7	1.11 ± 0.19	0.36 ± 0.25	0.69 ± 0.21	<0.001	<0.001	<0.001

Note. Cryo = cryopreserved; Vitrified = bulk droplet vitrified; RFU = relative fluorescence units.